INTERACTION BETWEEN PLATE AND LATERAL-TORSIONAL BUCKLING WITH REGARD TO RESIDUAL STRESSES

L. HEGEDŰS and M. IVÁNYI

Department of Steel Structures,
Technical University, H-1521 Budapest

Received November 29, 1984

Abstract

The complex of strain hardening of steel, occurring residual stresses, interaction of plate and member buckling significantly affects the stability condition of beam-columns. Theoretical results obtained by the energy method relying on the theory of plastic deformation match test results.

1. Introduction

1.1 Plastic methods are increasingly applied for the design of steel structures, still forwarded by "plastic design codes" issued in a number of countries, partly from economical considerations, partly from the consideration that failure safety of structures can only be examined by methods of plastic analysis.

"Plastic design codes" have been issued in several countries including Hungary.

The Department of Steel Structures, Technical University, Budapest had an important share in theoretical and experimental work underlying these specifications.

1.2 Analysis of the plastic load capacity of steel structures requires to meet a system of conditions of several subsystems referring either to material and geometry of the structure, residual stresses arising in manufacture, or to ways of loading, etc. A significant part of the system of conditions refers to stability phenomena, to interaction between stability and strength phenomena.

This study will mainly concern the interaction between plate and lateral-torsional buckling, as well as some factors of significance for the mentioned interaction.

2. Experimental investigations

2.1 Experimental investigations are essentially expected partly to supply physical background (often inspiration) needed to establish models for theoretical examinations, and partly to delimit the range of validity.

Our experiments involved measurements to determine:

a) plastic material characteristics of steel;

b) residual deformations;
c) load carrying capacities of members in compression, bending and eccentric compression.

ad a) Plastic material characteristics of steel have been determined in tensile tests on a total of 76 standard specimens of different plate thicknesses. Material testing results for specimen no. 21 are seen in Fig. 1.

ad b) Residual strains or stresses of welded I-sections have been determined by the sectioning method. Residual strains affect both strength and stability phenomena. Tests comprised determination of residual deformations of 32 different cross sections in all. Distribution of residual stresses in specimen no. 21 is seen in Fig. 2.

ad c) Load carrying capacities of members in compression, bending and eccentric compression have been tested by experimental methods. The testing program covered I-sections of two different outlines ($B/b = 0.6; 0.8$). Either of the two cases had four different web slendernesses, each of them with four flange widths (Fig. 3). Thereby a series comprised 32 specimens in all, each type was exposed to four different distributions of stresses. The experimental program involved testing of 132 specimens.

2.2 Results of tests and of theoretical analyses will be compared in Chapter 5.

3. Phenomena and effects

3.1 Strain hardening of steel has been determined from the uniaxial state of stress condition. Uniaxial state of stress condition of an elastic-ideally plastic material is seen in Fig. 4a, and of an elastic-strain hardening material in Figs 4b and c.

Material equations in the plastic range may be established either after the Hencky's theory of plastic deformation, or the Prandtl-Reuss theory of plastic yield [1].

For strain-hardening materials, the theory of plastic deformation yields the material law of a nonlinear elastic solid. The theory of plastic deformation cannot be generally considered as perfect, and the relevant results can only be accepted as approximations, but in the case of a so-called "simple load", if upon loading, stress components at any point of the solid grow in proportion to some parameter, material equations by Hencky yield theoretically exact results [2].

3.2 Distribution and value of residual stresses depend on several factors, including geometry, material quality, various manufacturing, technology processes (rolling, welding, straightening, etc.).

Distribution and value of residual stresses are mainly accessible to experimental methods [3]. Experimental investigations are bound to technical

difficulties, at the same time quantitative and qualitative (distributional) characteristics of residual stresses impose statistical analyses.

3.3 The problem of interactions will be illustrated by analysing the interaction between plate and lateral-torsional buckling on a simple example in-

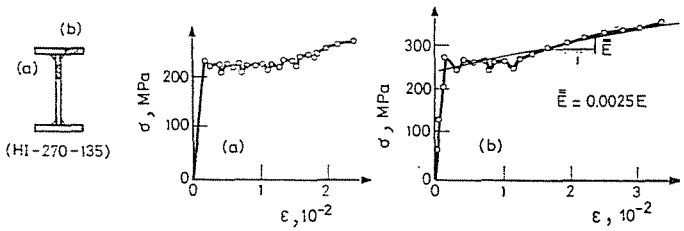

Fig. 1

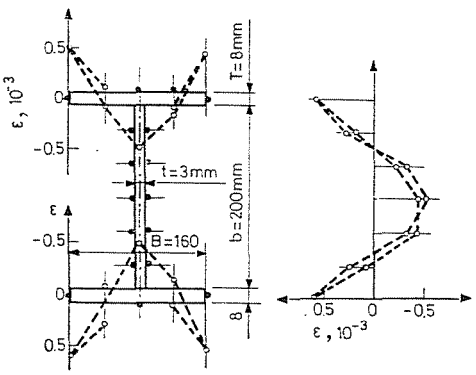

Fig. 2

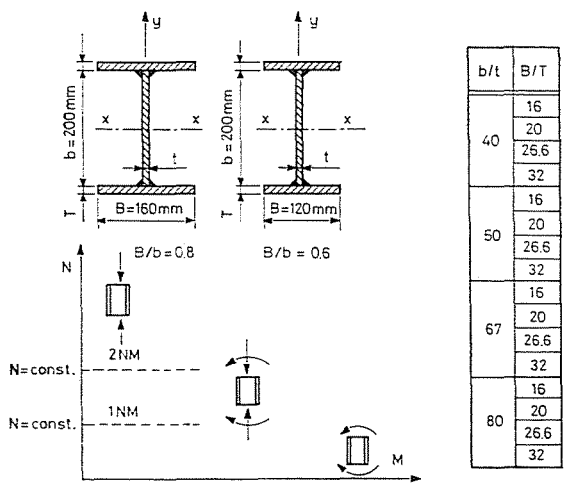

b/t	B/T
40	16
	20
	26.6
	32
50	16
	20
	26.6
	32
67	16
	20
	26.6
	32
80	16
	20
	26.6
	32

Fig. 3

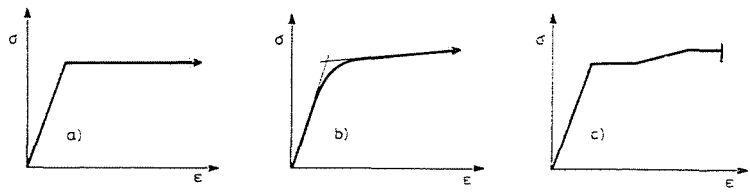

Fig. 4

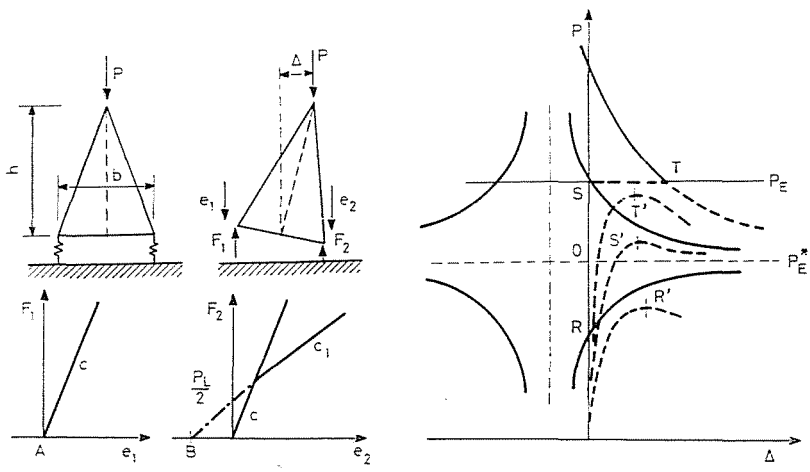

Fig. 5

volving the behaviour of the so-called "Shanley model" [4] (Fig. 5). The model is that of a rigid member in compression, supporting springs simulate behaviour of bar flanges, neglecting the effect of the web plate.

Spring no. 2 takes post-critical behaviour of the flange plate (after equilibrium bifurcation) by taking the characteristic curve of the spring into consideration. For a sufficiently high force P_L at flange buckling, both springs behave identically up to a relatively high force value, and the critical load of the model is:

$$P_E = \left(\frac{b^2}{2h}\right) c$$

the so-called Euler (critical) load. However, for $P_L < P_E$, at a force $P = P_L$, Δ will continuously increase, and the force-displacement curve of the perfect model tends to the force described by spring factors c and c_1:

$$P_E^* = \left(\frac{b^2}{2h}\right) \frac{2 \cdot c \cdot c_1}{c + c_1} .$$

At force $P_L = P_E^*$, an indifferent state of equilibrium develops (Engesser-Kármán's critical load).

Taking various forces P_L in the relationship above into consideration, load-displacement curves can be determined.

For $P_L < P_E^*$, equilibrium bifurcation of the perfect model is at R. For an imperfect model, this condition involves a curve reaching to peak R'. This is the case of "thin" plates. Imperfect characteristics are due to geometric imperfections, to the occurrence of residual stresses.

For $P_E^* < P_L < P_E$, the post-critical state is of unstable character, with the possibility of significant differences between load carrying capacity values of perfect and imperfect models. For $P_E = P_L$, member and plate bucklings are simultaneous. Points S and S' greatly differ, giving rise to the so-called "optimum erosion" [5].

Provided $P_E < P_L$, plate buckling affects only the condition of the perfect model after equilibrium bifurcation due to "lateral-torsional" bar buckling. Duly selecting the proportions, points T and T' may be made to belong to nearly identical load carrying capacities, and the imperfect model endowed with deformation capacity; this is the case of "thick" plates. Thereby in plastic design, the effect of plate buckling on the deformation capacity of a structural part or of the complete structure prevails.

4. Interaction between plate and lateral-torsional buckling

4.1 Recently, interaction between plate and lateral-torsional buckling has come to the foreground of interest. Analyses have been made using different models and methods. One solution of the problem applied folded plates [6],

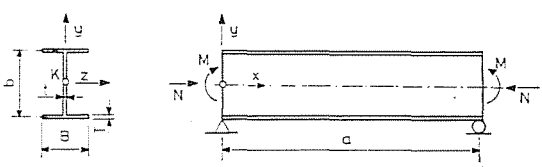

Fig. 6

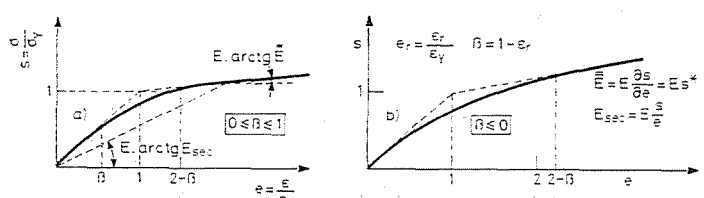

Fig. 7

[7]. The most current methods are the energy and the variational methods [8], [9]. Early in the '70s, the finite element method [10], [11], then the finite strip method [12], [13] have been introduced for the analysis of the interaction between plate and lateral-torsional buckling.

This paper will present an analysis based on the energy method, taking also the plastic state of the steel material into consideration. The bar is exposed to normal force and to constant bending moment, the procedure takes also the effect of residual stresses in the bar, due to the manufacturing technology, into consideration.

4.2 Geometry of the tested member is seen in Fig. 6. The member is simply supported at each end with regard to both bending and twisting.

The member material is assumed to be strain-hardening (Fig. 7); provided residual stresses σ_r are lower than the yield point σ_Y, relationship in Fig. 7a, otherwise that in Fig. 7b, will be applied. The transition between the elastic and the strain hardening ranges may be written in terms of a polynomial — assuming the residual strains to be of linear distribution.

Distribution of residual strains and stresses due to technology processes over the cross section is accounted for according to Fig. 8. Residual strains are assumed to be of linear distribution both in the flanges and the web, residual stresses arising in the cross section will be referred to this strain diagram according to the σ—ε diagram of the elastic-strain-hardening material.

Until the development of the critical state, strains due to loading will be considered to be of constant distribution in the flanges, and linearly varying in the web (Fig. 9a), thereby the loading can be described in terms of the strain in an extreme fibre and parameter α, and residual strains added, making up the load seen in the cumulative diagram in Fig. 9b.

Taking the α value constant in an actual analysis, a so-called "simple load" is obtained: axial load for $\alpha = 0$, bending for $\alpha = 2$, while $0 < \alpha < 2$ means combined effect of compression and bending.

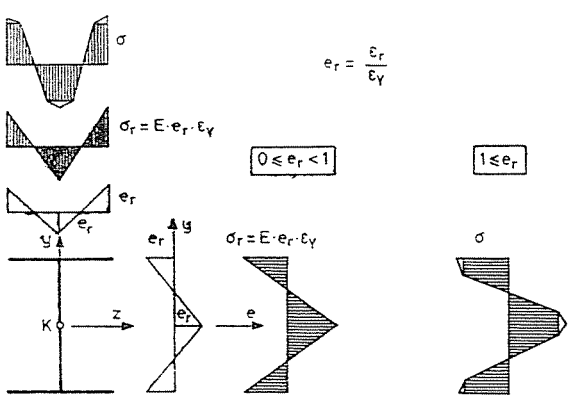

Fig. 8

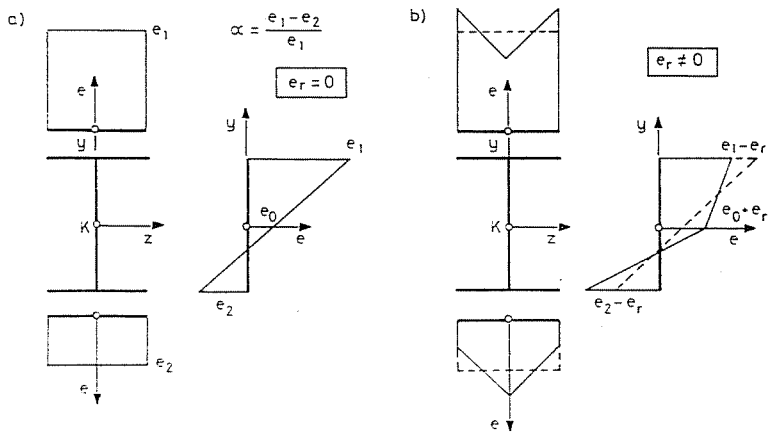

Fig. 9

4.3 Analysis of the examined phenomenon will make use of the theory of plastic deformation.

Taking the so-called Shanley phenomenon into consideration (i.e. inexistence of unloading parts, regions of equilibrium bifurcation in the plastic range), potential energy of the member can be written.

Relying on results by Bijlaard and Ilyushin, Stowell [14] has established the potential energy of the web plate:

$$U_w = \frac{1}{2}\int_0^a \int_{-\frac{b}{2}}^{\frac{b}{2}} \{D'[C_1(w'')^2 + (w^{\cdot})^2 + (w'')(w^{\cdot})] + (w^{\cdot})^2]\}\, dx\, dy$$

$$V_w = -\frac{1}{2}\int_0^a \int_{-\frac{b}{2}}^{\frac{b}{2}} t[\sigma_w (w')^2]\, dx\, dy$$

where $\sigma_w = E \cdot \varepsilon_Y \cdot s_w$

$$C_1 = \frac{1}{4} + \frac{3}{4}\frac{E_t}{E_{sec}} = \frac{s_w + 3s_w^* e_w}{4s_w}$$

$$D' = \frac{E_{sec} \cdot t^3}{12(1 - \nu^2)} = E\frac{s_w t^3}{9e_w} \qquad (\nu = 0.5)$$

$$w' = \frac{\partial w}{\partial x} \quad w^{\cdot} = \frac{\partial w}{\partial y} \quad s_w^* = \frac{\partial s_w}{\partial e_w}$$

The potential energy of flanges can also be written: if at

$$y = \pm \frac{b}{2} \qquad \varphi = -(w')$$

$$U_f = \frac{1}{2} \int_0^a \int_{(A_f)} E_{\text{sec}}\, \omega_0^2 (\varphi'')^2\, dA_f\, dx +$$

$$+ \frac{1}{2} \int_0^a (\varphi')^2 \int_{-\frac{B}{2}}^{\frac{B}{2}} G_{\text{sec}} \frac{T^3}{3} dz\, dx + \frac{1}{2} \int_0^a \int_{(A_f)} E_{\text{sec}} (w_0)^2 z^2\, dA_f\, dx$$

$$V_f = -\frac{1}{2} \int_{(A_f)} (\sigma_{f1} - \sigma_{f2}) \int_0^a \{(w_k')^2 - 2y(w_k')(\varphi') + y^2(\varphi')^2 + z^2(\varphi')^2\}\, dx\, dA_f$$

where $\sigma_{f1} = E \cdot \varepsilon_Y \cdot s_1 \qquad \sigma_{f2} = E \cdot \varepsilon_Y \cdot s_2$

$$G_{\text{sec}} = \frac{E_{\text{sec}}}{2(1+\nu)} = \frac{E_{\text{sec}}}{3} \qquad (\nu = 0.5)$$

Overall potential energy of the member:

$$\Pi = U_w + V_w + U_f + V_f.$$

4.4 A general shape of a cross section is seen in Fig. 10: K (centroid), 0 (torsion centre).

For a bisymmetrical cross section in the elastic range, centroid and torsion centre are coincident.

In the plastic range, the two points do not coincide, for an I-section (Fig. 11):

$$\int_{(A_f)} \sigma_\omega^{pl}\, dA_f = \varphi'' \int_{(A_f)} E_{\text{sec}}\, \omega_0\, dA_f = 0; \quad \bar{\omega} = 0$$

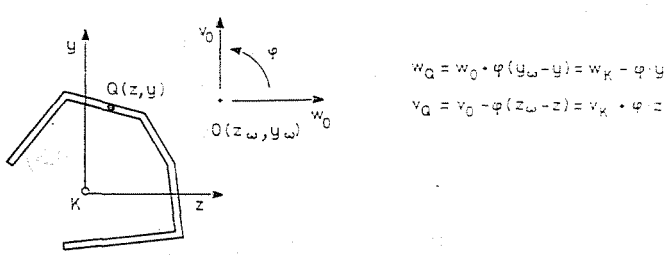

Fig. 10

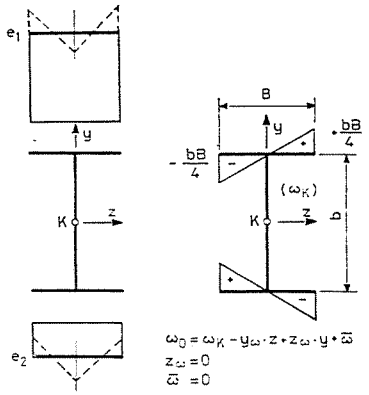

Fig. 11

$$\int_{(A_f)} \sigma_\omega^{pl} y \, dA_f = \varphi'' \int_{(A_f)} E_{sec} \omega_0 y \, dA_f = 0$$

$$y_\omega = \frac{\int_{(A_f)} E_{sec} \omega_k z \, dA_f}{\int_{(A_f)} E_{sec} z^2 \, dA_f}$$

$$\int_{(A_f)} \sigma_\omega^{pl} z \, dA_f = \varphi'' \int_{(A_f)} E_{sec} \omega_0 z \, dA_f = 0$$

$$z_\omega = 0$$

Effect of torsion centre migrating in the plastic range as a function of plastic deformation has been reckoned with in writing potential energies of flanges.

4.5 The critical state will be determined by varying function $w(x, y)$ as minimum of functional Π. The problem will be solved by the Ritz method. Let the deformed shape be:

$$w(x, y) = X(x) \cdot Y(y).$$

Taking boundary conditions of the member into consideration:
a) for a member with "pinned" end with regard to twisting:

$$X(x) = \sum_p \sin \frac{p \pi x}{a}$$

b) for a member with "fixed" end with regard to twisting:

$$X(x) = \frac{1}{2} \sum_p \left(\cos \frac{(p-1) \pi x}{a} - \cos \frac{(p+1) \pi x}{a} \right)$$

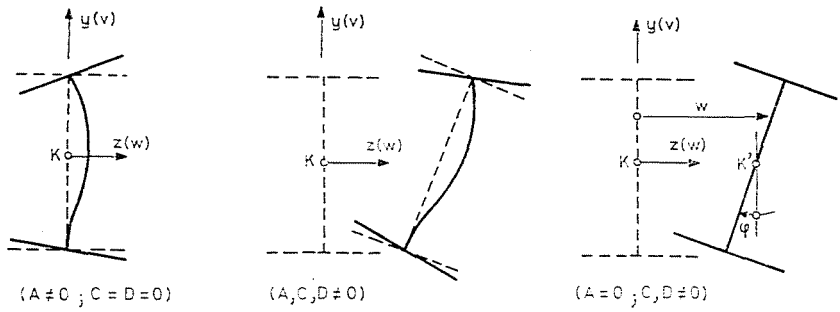

Fig. 12

Cross-sectional deformation is seen in Fig. 12, thus:

$$Y(y) = \sum_q A_{pq} \sin \frac{q\pi}{b}\left(y + \frac{b}{2}\right) + B_p \frac{y}{b} + C_p$$

Also, according to Fig. 12, the cases of plate buckling and of lateral-torsional buckling may be separately analyzed by means of coefficients A_{pq}, B_p and C_p.

Substituting derivatives of function $w(x, y)$ into the term of potential energy Π, specific strain value e_1 leading to critical state for a preassumed α can be found. This problem has been solved on a computer PDP 11/34. The program selects as many terms from the series of function $w(x, y)$ as needed for a deviation below 2% between values for n and $n + 1$ terms in the final result. In the examined cases, nine terms always sufficed.

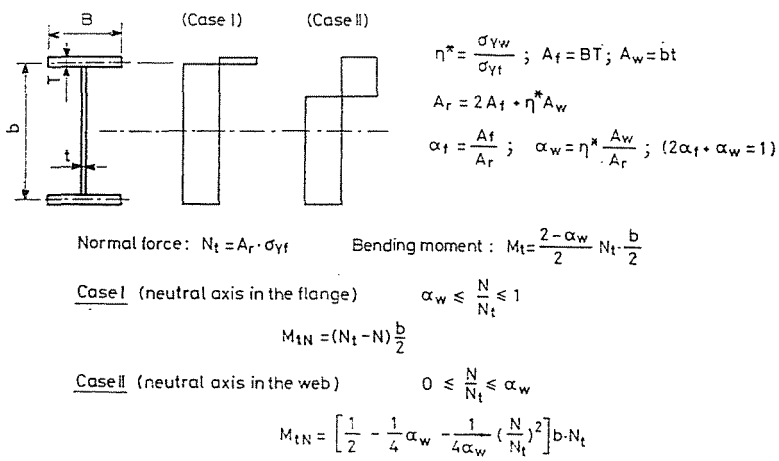

Fig. 13

5. Theoretical and experimental investigation results

5.1 In theoretical computations, geometrical imperfections and yield stress differences due to different plate thicknesses have been taken into consideration. Test results have been compared to load carrying capacities obtained on a rigid-ideally plastic material model (Fig. 13).

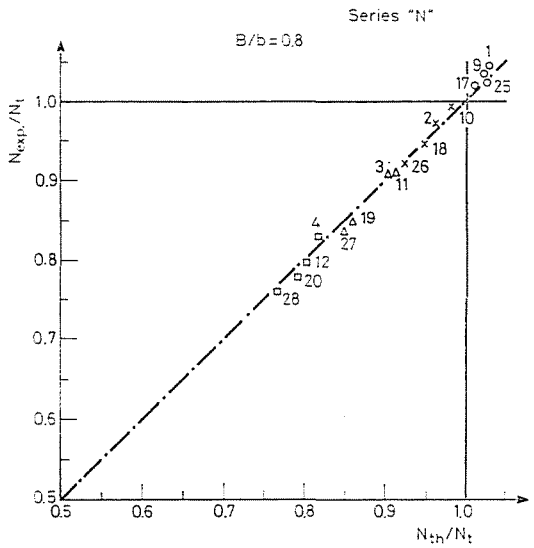

Fig. 14

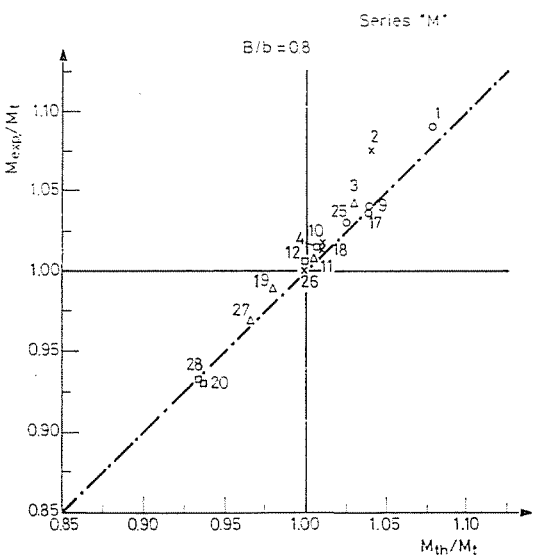

Fig. 15

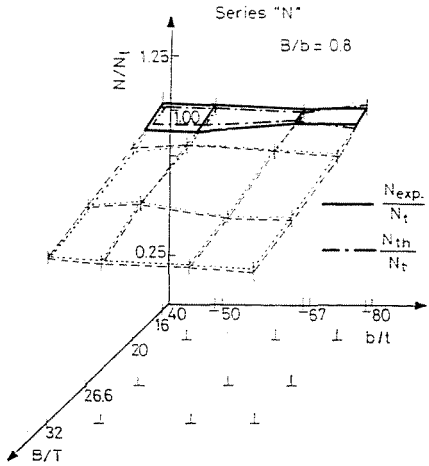

Fig. 16

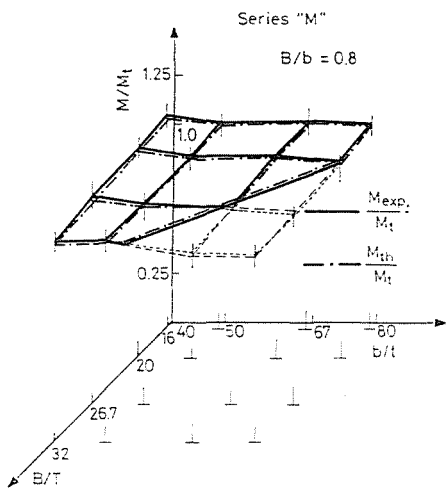

Fig. 17

5.2 Residual strains of welded I-sections have been determined, and measured values utilized in theoretical analyses.

In the plastic range, structural steel exhibits a yield "plateau" and strain hardening, approximated by a single, substitutive strain hardening modulus in the analysis.

5.3 Results are seen to agree in Figs 14 and 15 recapitulating results on specimens in pure compression and in pure bending for a ratio $B/b = 0.8$ of flange width to web depth. A similar agreement was found between experimental and theoretical results on specimens under eccentric load.

5.4 Load carrying capacity ratios depending on component plate slendernesses (B/T and b/t being width to thickness ratios of flange and web, respectively) are seen in Figs 16 and 17, pointing out plate proportions where the load carrying capacity determined from buckling coincides with that for the rigid-ideally plastic state. For an axial load, the flange slenderness prevails over the web plate slenderness (Fig. 16), while in pure bending (Fig. 17), both slendernesses act equally.

6. Examination of influences on the interaction

6.1 This theoretical method, experimentally qualifying as adequate, has been applied to examine plate buckling, lateral-torsional buckling, and their interaction, for a bar of typical cross section (Fig. 18).

The tested member was supported hinged for bending, and "fixed-end" for twisting. Residual strains have been assumed to be distributed as seen in the diagram, with values referred to the yield strain ($e_r = \varepsilon_r/\varepsilon_Y$).

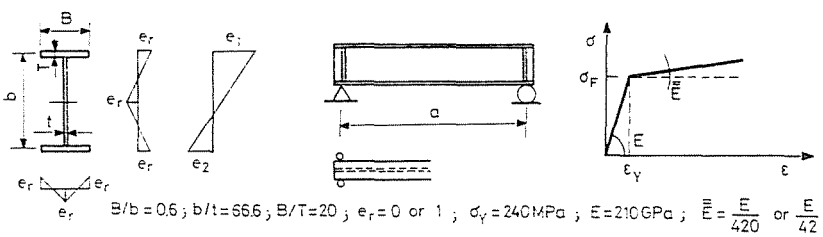

Fig. 18

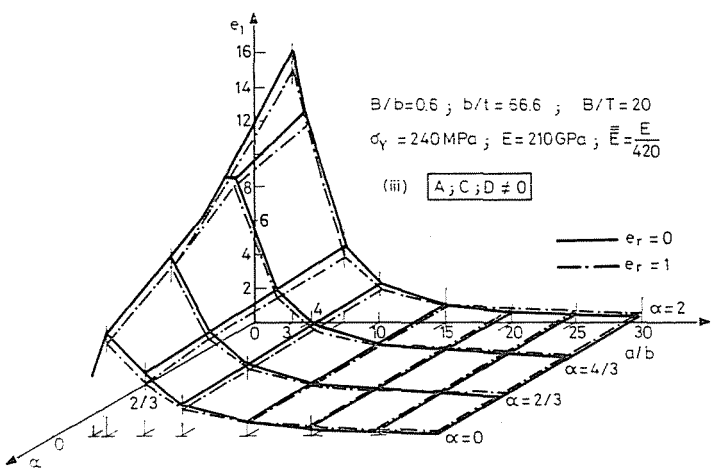

Fig. 19

The load has been described in terms of the relative strain of the extreme fibre in compression ($e_1 = \varepsilon_1/\varepsilon_Y$) and of parameter $\alpha = 1 - e_2/e_1$ to be determined from extreme fibre strains ($\alpha = 0$ in pure compression, $\alpha = 2$ in pure bending).

6.2 Analyses referred to the effects of member length, strain hardening modulus of steel material, residual strains, stresses and cross-sectional deformations (web buckling ($A \neq 0$; C, $D = 0$), lateral-torsional buckling ($A = 0$; C, $D \neq 0$), and combined (A, C, $D \neq 0$)).

Granting the simultaneous possibility of web buckling and lateral-torsional buckling, specific strain values e_1 typical of the indifferent state have been sought for preassumed values of load parameter α ($\alpha = 0$; 2/3; 4/3; 2). Variation of e_1 values vs. α and the a/b (span to web depth) ratio are seen in Fig. 19 for negligible residual strains ($e_r = 0$) and those corresponding to the yield stress ($e_r = 1$).

In knowledge of the stress/strain relationship, this diagram can be transformed into the function of specific values of member-end compressive and bending stresses (Fig. 20).

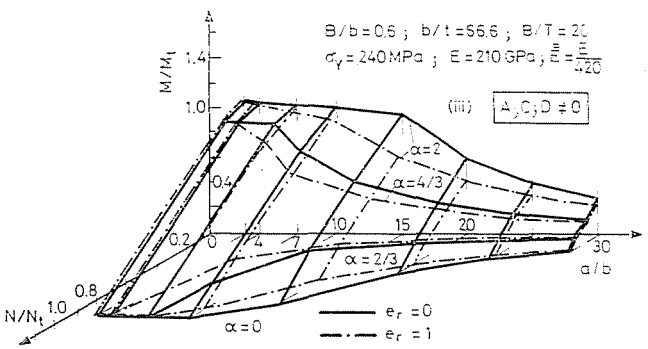

Fig. 20

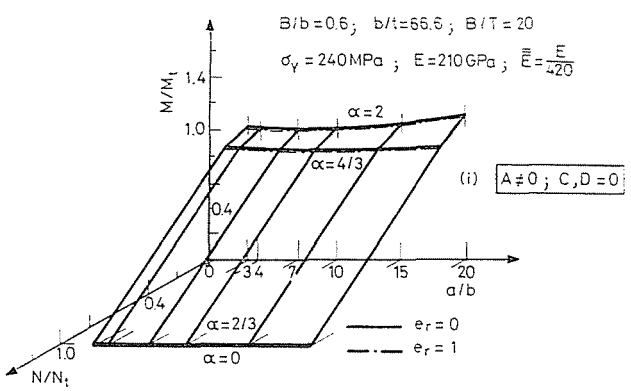

Fig. 21

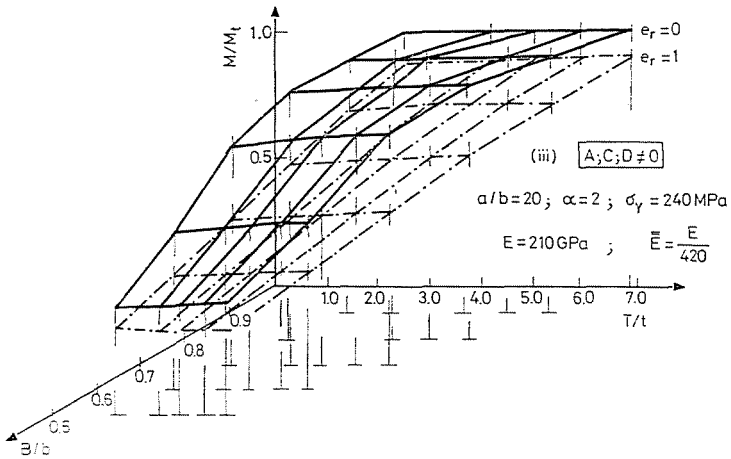

Fig. 22

6.3 The effect of the strain hardening modulus value has been examined utilizing results for ratios $\bar{\bar{E}}/E = 1/420$ and $1/42$. For the assumed geometries, at a span/depth ratio $a/b = 15$, the strain hardening modulus value practically did not affect the load capacity but below that it may be overwhelming.

6.4 Residual strains have the greatest effect at about a ratio $a/b = 15$, in the so-called "medium" slenderness range (with the assumed data, $\lambda = 87$).

6.5 Excluding the possibility of lateral-torsional buckling, relationship in Fig. 21 is obtained, where, with the geometry assumed, the minimum of the load carrying capacity is at a ratio $a/b = 7$ (assuming a length-wise wave). Excluding the possibility of web buckling, a diagram rather similar to Fig. 20 results, with a deviation distinct near $a/b = 7$.

6.6 As concerns the effect of bar geometry on load carrying capacity, for a ratio $a/b = 20$ usual in construction, and in pure bending, the ratio B/b of flange width to web depth was seen to markedly affect the load capacity (Fig. 22). The greatest load capacity decrease due to residual deformation was found at about $B/b = 0.7$.

References

1. KALISZKY, S.: Theory of Plasticity. (In Hungarian). Akadémiai Kiadó, 1975 Budapest.
2. KACHANOV, L. M.: Foundations of the theory of plasticity. North-Holland Publ. Co., Amsterdam—London, 1971.
3. PEITER, A.: Eigenspannungen I. Art. Michael Triltsch Verlag, 1966, Düsseldorf.
4. CROLL, I. G. A.—WALKER, A. C.: Elements of structural stability. Wiley, 1972, London.
5. THOMPSON, J. M. T.—HUNT, G. W.: A general theory of elastic stability. Wiley, 1973, London.
6. SUZUKI, Y.—OKUMURA, T.: Influence of cross-sectional distorsion on flexural-torsional buckling. Final Report IABSE, 1968, New York.
7. KOLLBRUNNER, C. F.—HAJDIN, N.: Die Verschiebungsmethode in der Theorie der dünnwandigen Stäbe und ein neues Berechnungsmodell des Stabes mit seinen ebenen deformierbaren Querschnitten. Publications, IABSE, *28*, *II.* 87 (1968).

8. FISCHER, M.: Das Kipp-Problem querbelasteter exzentrisch durch Normalkraft beanspruchter I-Träger bei Verzicht auf die Voraussetzung der Querschnittstreue. Der Stahlbau, *36*, 77 (1967).
9. SCHMIED, R.: Die Gesamtstabilität von zweiachsig außermittig gedrückten dünnwandigen I-Stäben unter Berücksichtigung der Querschnittsverformung nach der nichtlineare Plattentheorie. Der Stahlbau, *36*, 1 (1967).
10. RAJASEKARAN, S.—MURRAY, D. V.: Coupled local buckling in wide-flange beam-columns. Jrl. of Struct. Div. ASCE, *99*, No. ST6. 1003 (1973).
11. JOHNSON, C. P.—VILL, K. M.: Beam buckling by finite element procedure. Jrl. of Struct. Div. ASCE. *100*, No. ST3. 669 (1974).
12. HANCOCK, G. J.: Local, distortional and lateral buckling of I-beams. Jrl. of Struct. Div. ASCE. *104*, No. ST11. 1787 (1978).
13. HANCOCK, G. J.—BRADFORD, M. A.—TRAHAIR, N. S.: Web distortional and flexural-torsional buckling. Jrl. of Struct. Div. ASCE. *106*. No. ST7. 1557 (1980).
14. STOWELL, E. Z.: A unified theory of plastic buckling of columns and plates. NACA Technical Note, No. 1556 (1948).
15. IVÁNYI, M.: Interaction of Stability and Strength Phenomena in the Load Carrying Capacity of Steel Structures. Role of Plate Buckling. (In Hungarian.) Doctor Techn. Sci. Thesis, Hung. Ac. Sci., Budapest, 1983.

Dr. László HEGEDŰS
Prof. Dr. Miklós IVÁNYI
H-1521 Budapest